



Published in final edited form as:

J Am Chem Soc. 2012 October 10; 134(40): 16781–16790. doi:10.1021/ja307220z.

Identification and Characterization of the Echinocandin B Biosynthetic Gene Cluster from *Emericella rugulosa* NRRL 11440

Ralph A. Cacho¹, Wei Jiang³, Yit-Heng Chooi¹, Christopher T. Walsh^{3,*}, and Yi Tang^{1,2,*}

¹Department of Chemical and Biomolecular Engineering, University of California, Los Angeles, 420 Westwood Plaza, Los Angeles, CA 90095

²Department of Chemistry and Biochemistry, University of California, Los Angeles, 607 Charles E. Young Drive East, Los Angeles, CA 90095

³Department of Biological Chemistry and Molecular Pharmacology, Harvard Medical School, 200 Longwood Ave, Boston, MA 02115

Abstract

Echinocandins are a family of fungal lipidated cyclic hexapeptide natural products. Due to their effectiveness as antifungal agents, three semisynthetic derivatives have been developed and approved for treatment of human invasive candidiasis. All six of the amino acid residues are hydroxylated, including 4*R*,5*R*-dihydroxy-L-ornithine, 4*R*-hydroxyl-L-proline, 3*S*,4*S*-dihydroxy-L-homotyrosine, and 3*S*-hydroxyl,4*S*-methyl-L-proline. We report here the biosynthetic gene cluster of echinocandin B **1** from *Emericella rugulosa* NRRL 11440 containing genes encoding for a six-module nonribosomal peptide synthetase EcdA, an acyl-AMP ligase EcdI and oxygenases EcdG, EcdH and EcdK. We showed EcdI activates linoleate as linoleyl-AMP and installs it on the first thiolation domain of EcdA. We have also established through ATP:PPi exchange assay that EcdA loads L-ornithine in the first module. A separate *hty* gene cluster encodes four enzymes for *de novo* generation of L-homotyrosine from acetyl-CoA and 4-hydroxy-phenyl-pyruvate is found from the sequenced genome. Deletions in the *ecdA*, and *htyA* genes validate their essential roles in echinocandin B production. Five predicted iron-centered oxygenase genes, *ecdG*, *ecdH*, *ecdK*, *htyE*, *htyF*, in the two separate *ecd* and *hty* clusters are likely to be the tailoring oxygenases for maturation of the nascent NRPS lipohexapeptidolactam product.

Keywords

antifungal; nonribosomal peptide; lipopeptide; unnatural amino acids; genome mining

INTRODUCTION

Invasive candidiasis caused by opportunistic pathogenic strains of genus *Candida*, accounts for 17% of ICU-related infections, third highest after *Staphylococcus aureus* and *Pseudomonas* spp.-related infections.¹ Moreover, there has been a steady increase in the incidence of invasive candidiasis correlating with the increased use of immunosuppressants, broad-spectrum antibiotics, intravenous catheters and prosthetics and invasive clinical

Corresponding Authors: yitang@ucla.edu, christopher_walsh@hms.harvard.edu.

Additional bioinformatics data, *in vitro* assay results and spectra are found in the supplemental information.

This material is available free of charge via the Internet at <http://pubs.acs.org>.

procedures.²⁻³ Echinocandins, a family of lipohexapeptides that prevent fungal wall synthesis through noncompetitive inhibition of 1,3- β -glucan synthase, rapidly rose to the top ranks of antifungal agents due to their activity against a wide range of *Candida* spp., in particular azole-resistant strains, and are significantly less toxic compared to Amphotericin B.⁴⁻⁵

As the first echinocandin discovered, Echinocandin B **1**, was isolated from *Aspergillus nidulans* var. *echinulatus*⁶ and *A. nidulans* var. *roseus* NRRL 11440.⁷ While **1** and family members subsequently isolated, such as pneumocandin A₀ **4**,⁸ aculeacin,⁹ cryptocandin,¹⁰ and mulundocandin¹¹, show anti-*Candida* activity, the hemolytic properties of natural echinocandins prevented their use as therapeutics. Derivatization of **1** and **4**, especially in the fatty acid moiety, led to the development of cilofungin **2**,¹²⁻¹³ anidulafungin **3** (Eraxis, Pfizer),¹⁴ caspofungin (Cancidas, Merck and Co) **5**,¹⁵ and micafungin **6** (Mycamine, Astellas Pharma)¹⁶ (Scheme 1) that have less hemolytic properties while retaining the bioactivity of their parent compound. For example, **3**, a semisynthetic derivative of **1** containing a substituted terphenyl acyl chain, was approved by the FDA in 2006.^{14,17}

In addition to their antifungal activity, echinocandins reflect interesting biosynthetic features in their structures. Aside from the long chain fatty acyl amide, the presence of nonproteinogenic amino acids *4R*, *5R*-dihydroxyl-L-ornithine, *3S*-hydroxyl, *4S*-methyl-L-proline, *4R*-hydroxyl-L-proline and *3S*, *4S*-dihydroxyl-L-homotyrosine suggests echinocandins are synthesized by nonribosomal peptide synthetases (NRPSs). An intriguing feature of echinocandins is the presence of multiple alcohol and diol groups within the scaffold as a result of the incorporation of these unnatural residues; most distinct of these hydroxyl groups are at C δ of L-ornithine which creates a hydrolytically labile hemiaminal in the macrocycle¹⁸⁻¹⁹ and the vicinal diol found in *3S*, *4S*-dihydroxy-L-homotyrosine. It is noted that enzymatic C δ -hydroxylation of L-ornithine is a particularly novel and challenging reaction due to the presence of the neighboring amine. Because of this unstable linkage, the total synthesis of **1** has not been demonstrated so far. Only simpler versions without the hydroxyl groups in the L-ornithine position, such as echinocandin D, have been synthesized and used in SAR studies.²⁰⁻²²

Despite the medical importance and intriguing structural motifs in echinocandin, the genetic and molecular basis for the biosynthesis of this family has remained unknown to date. The enzymology (sequence, specificity, type of oxygenase) behind this multitude of hydroxylation steps is also unresolved. *A. nidulans* var. *roseus* NRRL 11440 (ATCC 58397) is an industrially important strain that produces **1**, which is a precursor for the semisynthetic **3** (Scheme 1). A polyphasic characterization showed that this strain should belong to the *Emericella rugulosa* species and henceforth, we use that nomenclature here.²³ In this study, we report the discovery of the gene cluster of **1** in this strain through gene deletion of a multimodular NRPS and biochemical characterization of the enzymes involved in the lipoinitiation process. Through gene deletion and chemical complementation, we have also uncovered the separate gene cluster responsible for the biosynthesis of L-homotyrosine in the peptide scaffold of **1**.

RESULTS

Whole Genome Sequencing and Analysis of NRPS Gene Clusters of *Emericella rugulosa* NRRL 11440

Whole genome shotgun sequencing of *E. rugulosa* NRRL 11440 was performed using Illumina HiSeq2000 to generate ~17 Gbp of sequence. Assembly of the sequence reads generated 433 contigs with N50 length of 235,313 bases (See Table S1). The total length of

the 433 contigs amounts to 32,224,016 bases, which is slightly larger than the genome size of the previously sequenced *A. nidulans* A4 strain of ~31 Mb.²⁴

Using the first adenylation (A) domain of the enzyme TqaA (accession number: ADY16697) from the tryptoguanine pathway²⁵ as BLAST query, we were able to find 26 putative NRPS genes in *E. rugulosa* (Table S2). Four out of the twenty-six NRPSs, which we denoted as ErNRPSs, are NRPSs with five or more modules. Two of these four ErNRPSs, annotated as ErNRPS99 and ErNRPS57, are also found in the model fungi *A. nidulans* A4 that does not produce **1**. ErNRPS99 is likely a homolog of EasA found in the biosynthesis of emericellamide²⁶ due to the high shared sequence identity between the two. ErNRPS57, on the other hand, contains a terminal reductive domain (R) similar to what is found in peptaibol synthetases.²⁷ Thus, this leaves ErNRPS284 and ErNRPS123 as echinocandin synthetase candidates. ErNRPS284 (Table S2) contains five modules, which are insufficient for catalyzing the formation of the hexalipopeptide scaffold of **1** based on the colinearity hypothesis.²⁸ On the other hand, the six-module ErNRPS123 (799 kDa), which is annotated as *ecdA*, has the correct number of modules necessary for the assembly of **1**. However, performing A domain selectivity prediction using NRPS predictor²⁹ offered little confirmation that this is the correct echinocandin NRPS, with only the third A domain prediction (L-proline) matching the corresponding amino acid in **1** (L-proline or 4*R*-hydroxyl-L-proline) (Table S3). Further bioinformatics analysis of the domain architecture of EcdA, as well as the genes within the *ecd* cluster, gave indications that this is most likely the correct gene cluster that is consistent with some of the expected biosynthetic transformations required for the assembly of **1**. First, EcdA has a terminal condensation domain (C_T) that has been shown to catalyze the cyclization of NRPS products in fungi³⁰, in agreement with the anticipated macrocyclization of the hexapeptide. Furthermore, in proximity to *ecdA* is *ecdI* (Figure 1A and Table 1), an acyl-AMP ligase homolog gene, giving a plausible route for lipo-initiation of the NRPS. In addition, other genes adjacent to *ecdA* encode putative non-heme iron, α -ketoglutaratedependent oxygenases (*ecdG* and *ecdK*), and a cytochrome P450 heme-iron-dependent oxygenase (*ecdH*) (Table 1), indicating that the nascent NRPS product may undergo several oxygenation steps, as anticipated for the biosynthesis of **1**. Other genes flanking the putative *ecd* cluster encode a fungal transcription factor gene (*ecdB*), three transporter protein genes (*ecdC*, *ecdD* and *ecdL*), a glycosyl hydrolase gene (*ecdE*), a glycosidase gene (*ecdF*) and a gene encoding for a protein with no predicted conserved domain (*ecdJ*). Interestingly, genes encoding the biosynthesis of unnatural amino acids such as L-homotyrosine are not present in the vicinity of *ecd* gene cluster, but are found to reside elsewhere on the genome (see below).

Verification of the role of *ecdA* in the biosynthesis of **1**

To confirm the production of **1**, *E. rugulosa* was grown in Medium 2 and the metabolite extracted from the fermentation broth in the same manner as previously described.⁷ High resolution LCMS trace of the extracted metabolites shows a peak at 17.6 min with *m/z* of 1042.5700 [M+H-H₂O]⁺ corresponding to the theoretical mass-to charge ratio of **1** (*m/z* = 1042.5707 [C₅₂H₈₁N₇O₁₆+H-H₂O]⁺) (Figure 1B). Purification and subsequent characterization by NMR (Table S3 and Figure S13–S16) and comparison with authentic standard (Figure S1) verified that the compound is indeed **1**.

To verify whether the *ecd* cluster is responsible for the production of **1**, we developed a gene deletion method for *E. rugulosa* based on previous methods for *A. nidulans* A4,³¹ using the glufosinate resistance gene *bar* as selection marker (See Materials and Methods).³² A gene deletion cassette containing portions of *ecdA* internally disrupted by the *bar* gene driven by the *tpC* promoter was introduced into *E. rugulosa* protoplasts via PEG-mediated transformation and the resulting glufosinate-resistant strains were selected. A bioassay-

guided knockout screening was developed in which individual fungal colonies are spotted on plates pre-inoculated with *C. albicans*. Approximately 100 mutants were screened by both loss of anti-*Candida* activity, and PCR-based screening using a *bar* gene primer and a primer found outside the knockout cassette. One mutant ($\Delta ecdA$ I-16) was isolated which lost the ability to inhibit the growth of *C. albicans* (Figure S2) and also showed the correct PCR-amplified product (Figure S3). LCMS analysis of the extracted metabolites after 7 days of growth showed no production of **1** (Figure 1B), suggesting that EcdA is the NRPS responsible for the biosynthesis of **1**.

Characterization of the Adenylation domain (A) of the First Module of EcdA

Guided by the results of the gene knockout of *ecdA*, we proceeded to determine the amino acid specificity of the first A domain of EcdA by cloning the initiation module of EcdA, which is fused to a thiolation domain (T_0) that is likely the site of lipid attachment (EcdA-M1, T_0CAT_1). The 130 kDa protein was expressed in *Escherichia coli* BL21(DE3) cells to a final titer of ~20 mg/L and purity of >95% (Figure S4). Amino acid-dependent ATP-[^{32}P]-PPi exchange assay with 2 μ M of EcdA-M1 at ambient temperature and incubation time of 30 minutes showed that A_1 could activate L-ornithine (L-Orn) and (4*R/S*)-4-hydroxyl-L-ornithine (4-OH-L-Orn). D-ornithine and other amino acids with basic side chains such as L-lysine and L-arginine were not activated (Figure 2A). Full kinetic analysis shows that L-Orn ($k_{cat} = 43.5 \pm 1.9 \text{ min}^{-1}$, $K_M = 45.4 \pm 8.8 \mu\text{M}$) is about a 500-fold better substrate than 4-OH-L-Orn ($k_{cat} = 5.6 \pm 0.2 \text{ min}^{-1}$, $K_M = 2.7 \pm 0.3 \text{ mM}$) as judged by k_{cat}/K_M ratios (Figure 2B and 2C), suggesting that oxidation at $C\gamma$ of L-ornithine most likely occurs after loading of L-Orn to T_1 . The activation of L-Orn by the first module of EcdA further supports the link between the NRPS and the biosynthesis of **1**.

EcdI catalyzed Lipo-initiation of EcdA

The addition of the lipid chain in the biosynthesis of lipopeptides, also known as lipo-initiation^{33–34}, is a critical step not only because it connects the fatty acid pool and NRPS biosynthesis, but also due to the importance of the lipid to the antimicrobial activities.¹⁴ Several mechanisms exist in activating and transferring the lipid chain to the NRPS.³⁴ These include fusion of a fatty acid synthetase (FAS)-like module to the N-terminus of a NRPS (mycosubtilin)³⁵; and transfer of the lipid chain to a dissociated T domain (daptomycin)^{36–37} or coenzyme A (surfactin)³³ by a fatty acyl ligase, followed by condensation with an aminoacyl adenylyate catalyzed by the first C domain. Since EcdA only contains six A domains, one for each of the residues in the hexapeptide scaffold, we reasoned that EcdI, containing an AMP-binding domain might be responsible for the formation of the activated form of linoleic acid and its transfer to the T_0 domain of EcdA. To test this hypothesis, we cloned EcdI into an *E. coli* expression vector and expressed the N-terminal His-tagged protein in BL21(DE3) with a titer of ~30mg/L and purity of ~95% (Figure S5). Using the purified phosphopantetheinyl transferase Sfp from *Bacillus subtilis*,³⁸ we converted *apo* EcdA-M1 into its *holo* form *in vitro*. After co-incubation of *holo* EcdA-M1 with EcdI, ATP and [^{14}C]-linoleic acid, the assay mixture was analyzed using SDS-PAGE and autoradiography. The autoradiogram shows a strong radiolabeling of the 130 kDa band, indicating that the ^{14}C -linoleic acid is covalently bound to EcdA-M1 (Figure 3A). In contrast, in the absence of EcdI, ATP or Sfp, nearly no labeling of EcdA-M1 can be detected, confirming the proposed mechanism (Figure 3C). Quantification of the radiolabel suggests that ~30% of EcdA-M1 is loaded with the labeled substrate (Figure 3B), consistent with fractional stoichiometries seen in other labeling studies.^{39–40}

To pinpoint which of the two thiolation domains in EcdA initiation module (T_0CAT_1) is acylated by the linoleoyl starter unit in the presence of EcdI, single mutations to the active site serines in the two thiolation domains were made. The S47A mutant ($T_0^*CAT_1$) prevents

phosphopantetheinylation of the initiation T domain, but leaves the T₁ domain available for conversion into the holo form that should be capable of undergoing covalent loading with [¹⁴C]-L-ornithine. Conversely, the corresponding S1127A mutant (T₀CAT₁*) will not be phosphopantetheinylated at T₁ but should be able to load [¹⁴C]-linoleate. Both the S47A and the S1127A mutants were expressed from *E.coli* BAP1,⁴¹ which coexpresses Sfp for thiolation domain phosphopantetheinylation (thus no Sfp preincubation is required) (Figure S6). As shown in Figure S7, [¹⁴C]-linoleate is loaded onto the T₀CAT₁* but not the T₀*CAT₁ variant of the EcdA initiation module, as assessed by both autoradiography and by radioactive counting of protein precipitated via addition of trichloroacetic acid. The complementary result is seen for [¹⁴C]-L-ornithine covalent loading in which T₀*CAT is labeled but T₀CAT₁* is not (Figure S8). The relatively low amount of L-Orn radioactivity may reflect lability of the thioester due to the attack by the N γ of the ornithine side chain to the activated carbonyl carbon followed by the subsequent release of the cyclic δ -lactam, a known propensity of ornithine thioesters.⁴²

In previously characterized lipopeptide NRPSs, the incorporation of fatty acids into the assembly line requires the formation of either acyl-CoA³³ or acyl-AMP³⁶ prior to loading onto the NRPS. To explore the mechanism of linoleic acid activation by EcdI, we removed excess CoA after conversion of *apo* EcdA-M1 to its *holo* form, followed by addition of 0, 0.5 or 5.0 mM CoA to the assay. The reaction rates for the acyl loading step, as determined by the fraction of EcdA-M1 loaded with labeled substrate at different time points, are essentially the same (Figure S9), ruling out the CoA-dependent mechanism and indicating that the acyl-AMP is directly transferred to EcdA-T₀ by EcdI (Figure 3C).

In order to probe the substrate specificity of EcdI, we coincubated *holo*-EcdA-M1 with alternative acyl substrates. Palmitic acid (C-16) showed similar degree of loading to EcdA-M1 compared to linoleic acid (27% vs. 30 % for linoleic acid). Decreasing the length of the acyl chain to C-10 ([¹⁴C]-decanoic acid), on the other hand, dramatically reduced the loading of EcdA to ~8% at time points where the loading of linoleic acid reaches saturation. Nevertheless, this range of fatty acyl chain lengths that can be transferred to EcdA-M1 indicates there is room for incorporation of alternative lipid starter molecules into the structure of **1**. Incubation of EcdI and EcdA-M1 with non-fatty-acid substrate such as benzoic acid, an aryl carboxylate, did not show covalent loading onto T₀ (Figure S10).

Discovery of the L-homotyrosine biosynthetic gene cluster

One of the characteristic features of the echinocandin family is the presence of nonproteinogenic 3*S*, 4*S*-dihydroxyl-L-homotyrosine in the 4th amino acid position of the cyclic hexapeptide. This residue is derived from the dihydroxylation of L-homotyrosine either prior to, or after incorporation into the peptide scaffold. It was previously shown that L-homotyrosine in the scaffold of **4** is derived from the condensation of 4-hydroxyphenylpyruvate and acetate to form 2-(4-hydroxybenzyl)-malate.⁴³ Likewise, the biosynthesis of L-homophenylalanine in watercress plants is proposed to follow a pathway analogous to leucine biosynthesis,⁴⁴ beginning with the condensation of acetyl-CoA and phenylpyruvate to form benzylmalic acid. In order to find putative 2-(4-hydroxybenzyl)-malate synthase (HBMS) that may be involved in L-homotyrosine biogenesis, we searched the *E. rugulosa* genome for genes encoding the functionally analogous isopropyl-malate synthase (IPMS), the enzyme that catalyzes the condensation of α -ketovalerate with acetyl-CoA in leucine biosynthesis. We used the IPMS gene from *Mycobacterium tuberculosis* (accession number: MT3813) as BLAST query. Two significant hits were found, ErIPMS48 and ErIPMS66, both of which are found outside the contig containing the *ecd* gene cluster. ErIPMS48 shares 99% protein sequence identity to the predicted *A. nidulans* A4 housekeeping IPMS (AN0804) as well as >85% identity to predicted IPMS in other ascomycetes, suggesting that

this gene encodes for the actual IPMS involved in leucine biosynthesis in *E. rugulosa*. On the other hand, the ErIPMS66 protein sequence has a lower similarity to AN0804 (43% protein identity), while such a second IPMS homolog is not present in *A. nidulans* A4. Downstream of ErIPMS66 (designated as *htyA*) are genes putatively encoding a transaminase (*htyB*), a 3-isopropyl-malate dehydrogenase homolog (*htyC*), and an isopropyl-malate isomerase homolog (*htyD*), all possibly involved in biosynthesis of L-homotyrosine (Table 2 and Figure 4A). Moreover, the presence of immediately upstream genes encoding for a predicted nonheme iron, α -ketoglutarate-dependent oxygenase (*htyE*) and cytochrome P450 oxygenase (*htyF*) are consistent with the requirement of C γ and C δ hydroxylation of L-homotyrosine in **1**. Thus, we reasoned that the gene cluster, here designated as *hty*, may be responsible for the biosynthesis of L-homotyrosine in *E. rugulosa*.

To confirm this hypothesis, we genetically disrupted the *htyA* gene in the same manner as for construction of $\Delta ecdA$. Screening of ~100 colonies yielded 3 PCR-positive mutants (Figure S11). All three $\Delta htyA$ mutants lost the ability to inhibit the growth of *C. albicans* under screening conditions (Figure S2), accompanied by the loss of production of **1** (Figure 4B). To chemically complement the $\Delta htyA$ mutant, 0.1 mg/mL of L-homotyrosine were supplemented to the growth media. As expected, adding free homotyrosine restored the ability of the mutant to inhibit *Candida* (Figure S2), as well as the production of **1** (Figure 4B) to wild type levels. As a negative control, feeding of L-homotyrosine to $\Delta ecdA$ I-16 mutant did not restore the production of **1** (Figure S1). Therefore, based on whole genome sequencing, we were able to identify a separately located gene cluster that is responsible for the biosynthesis of an unnatural amino acid building block for the *ecd* pathway.

Based on the putative functions of HtyA-D (Table 2), the biosynthesis of L-homotyrosine is predicted to be as follows (Figure 4C): 4-hydroxy-phenylpyruvate undergoes an aldol-type condensation by HtyA with the C-2 of acetyl-CoA followed by the release of CoA to form 2-(4-hydroxybenzyl)-malate. This is followed by isomerization of 2-(4-hydroxybenzyl)-malate to 3-(4-hydroxybenzyl)-malate by HtyD. Thereafter, 3-(4-hydroxybenzyl)-malate undergoes decarboxylation and oxidation to form 2-oxo-4-(4-hydroxybenzyl)-butanoic acid, coupled to reduction of NAD⁺ to NADH by HtyC. The product then undergoes transamination catalyzed by HtyB to form L-homotyrosine. The closest homologs of HtyA-D is found in a four gene cassette from *Alternaria alternata* that is predicted to catalyze the formation of 2-amino-4-phenyl-valeric acid (APVA) in AM-toxin.⁴⁵ Interestingly, this suggests that the HtyA-D homologs in the AM-toxin gene cluster must perform two cycles of the α -ketoacid elongation to afford APVA.

DISCUSSION

Echinocandins are a family of antifungal cyclic lipopeptides from ascomycetes. Through the sequencing of the genome of *E. rugulosa* NRRL 11440 and subsequent bioinformatics analysis of NRPS genes, we have identified *ecdA*, encoding a 799 kDa six module NRPS, which is confirmed by gene deletion to be required for production of **1**. The *ecd* gene cluster is flanked by two microsyntenic blocks belonging to two different chromosomes in *A. nidulans* A4. Upstream of the *ecd* cluster are a group of genes that are syntenic to genes found in Chromosome VII of *A. nidulans* A4 while the genes found downstream of the cluster is syntenic to genes found in *A. nidulans* A4 Chromosome V (Figure S12). This suggests that a chromosomal translocation occurred when *E. rugulosa* NRRL 11440 and *A. nidulans* A4 diverged from their common ancestor.

Another interesting result revealed by the study is the separation of the *ecd* gene cluster and the L-homotyrosine biosynthetic genes. By adding the distance to the nearest end of their respective contigs, the minimum distance between the two clusters is ~42.5 kb, assuming

that both clusters are located in the same chromosome (Figure S12). Moreover, similar to the phenomenon seen in the *ecd* gene cluster, the *hty* gene cluster is flanked by microsyntenic blocks from two different *A. nidulans* A4 chromosomes; upstream of *hty* cluster are genes that are syntenic to genes from Chromosome VII of *A. nidulans* A4 while downstream are genes that are syntenic to genes found in the *A. nidulans* A4 Chromosome VI (Figure S12). This chromosomal translocation in the *E. rugulosa* genome, in comparison to *A. nidulans* A4 genome, also prevents us from mapping the *hty* and *ecd* gene cluster in relation to the *A. nidulans* A4 chromosomes. While separation of the biosynthetic genes for **1** is unusual, it is not unprecedented. Examples of the separation of secondary metabolite biosynthetic genes in fungi are found in the dothistromin pathway in *Dothistroma septosporum*⁴⁶, the convergence of the orsellinic acid and anthrone biosynthetic pathways in *A. nidulans* to form spiroanthrones,⁴⁷ the austinol and dehydroaustinol pathways in *A. nidulans*,⁴⁸ and the putative tryptoquivaline pathway in *A. clavatus*, which is a feature identified after comparison to the closely related tryptoquialanine pathway in *Penicillium aethiopicum*.²⁵

Due to the size of the full-length EcdA, which is a formidable challenge for *in vitro* evaluation, we dissected the EcdA initiation module to establish the predicted specificity for L-ornithine activation by A₁. The ~130 kDa, four domain (T₀CAT₁) EcdA initiation module (EcdA-M1) was expressed from *E. coli*. Determination of selectivity of A₁ by amino acid-dependent ATP-[³²P]-PPi exchange assay established L-ornithine as the most likely substrate. Heterologous expression of EcdA-M1 and EcdI, an acyl-AMP ligase homolog, allowed us to investigate the mechanism of lipo-initiation of EcdA. Co-incubation of EcdA-M1 with EcdI, ATP and [¹⁴C]-linoleic acid indicated loading of linoleic acid to the initiation T₀ domain of EcdA. While much is known regarding the lipoinitiation strategies of the bacterial NRPS's,^{33–37} this study presents the first *in vitro* characterization of the lipo-initiation of fungal NRPS. In comparison to the bacterial NRPS systems, EcdI acts analogously to DptE in daptomycin biosynthesis:³⁶ each adenylates the fatty acid substrate which is subsequently transferred to the initiation T₀ domain. The difference between the two systems is that the acceptor thiolation domain is standalone to the NRPS DptA in daptomycin biosynthesis but is fused at the N-terminal of EcdA for the biosynthesis of **1**. Hence it is expected that the smaller EcdI requires interaction with a thiolation domain that is part of a multimodular megasynthetases. This appears to be a commonly employed strategy among fungal PKSs and NRPSs, in which smaller enzyme partners are recruited to interact with the thiolation and acyl carrier protein domains.^{49–50} Currently, semisynthesis of echinocandins used for medical use such as **3** and **6** require the biological deacylation of their parent compound via feeding to separate cultures of *Actinoplanes* spp. followed by chemical reacylation using protective chemistry.^{12,14} Thus, deciphering the lipo-initiation strategy may also enable the engineered biosynthesis of approved derivatives of **1** containing alternative lipid groups.

The presence of acyl-AMP ligase homolog gene *ecdI* within the *ecd* gene cluster led us to investigate whether other organisms, in particular filamentous fungi, also have clustering of genes encoding an acyl-AMP ligase and an NRPS with an N-terminal T₀ domain. A search in the NCBI database revealed five genes for fatty-acyl-AMP ligase that share identity 39% with EcdI and are clustered with genes of NRPS with an initiation T₀ domain (Table S6). Moreover, four of the five EcdI homolog genes are also clustered with highly-reducing PKS genes in addition to NRPS genes, further hinting that these gene clusters may encode for lipopeptide biosynthetic enzymes. Furthermore, *easD* from *A. nidulans*, the only characterized out of the five fatty acyl-CoA ligase genes, is shown to be involved in the biosynthesis of emericellamide. The emericellamide synthetase EasA, however, requires an additional acyltransferase EasC for lipo-initiation.²⁶ Such an acyl-transferase is notably

missing in the *ecd* gene cluster and is now proven not to be required for the linoleic acid loading in our *in vitro* assays.

Based on the results of the lipo-initiation by EcdI and determination of the selectivity of A₁, we can propose one possible pathway for the biosynthesis of **1** (Scheme 2): linoleoyl-AMP, produced by EcdI, is transferred to the initiation T₀ of EcdA. The linoleoyl-S-phosphopantetheinyl-T₀ is sequentially extended with L-ornithine, L-threonine, L-proline, L-homotyrosine, L-threonine and 4*S*-methyl-L-proline to form the linear hexapeptide. Thereafter, the terminal condensation (C_T) performs macrocyclization of the NRPS product³⁰ and the cyclic scaffold **7** is released from EcdA. In this pathway, in which all the hydroxylation reactions are proposed to occur following completion of the cyclic peptide, the unhydroxylated precursor **7** will undergo six rounds of hydroxylation. In congruence to modification of the residues found in **1**, five hydroxylase genes (*ecdG*, *ecdH*, *ecdK*, *htyE* and *htyF*) are embedded within the *ecd* and *hty* clusters. At this point, it is not possible to assign the hydroxylases based on sequence alone, as all are proposed to act on *sp*³ hybridized carbon atoms. It was previously shown that L-proline hydroxylation to 4*R*-hydroxyl-L-proline in protein scaffolds is catalyzed by a non-heme iron, α -ketoglutarate dependent oxygenase.⁵¹ Thus it is likely that the hydroxylation of L-proline in **1** might be catalyzed by any of EcdG, EcdK or HtyE. However, the possibility that a P450 oxidase such as EcdH or HtyF can catalyze the reaction cannot be excluded. On the other hand, the formation of vicinal diols to give the 4*R*,5*R*-dihydroxyl-L-ornithine and 3*S*,4*S*-dihydroxyl-L-homotyrosine residue are more novel compared to that of the modified proline, and may each require two hydroxylases to separately install the two hydroxyl groups. Due to the lability of the resulting hemiaminal,¹⁸ we anticipate that C δ hydroxyl group in L-ornithine must be installed after peptide macrocycle formation, and is likely the last step in the oxidative tailoring cascade. An equally likely pathway to **1** is that some of the amino acids are hydroxylated prior to incorporation into the hexapeptide. The most plausible candidate for this scenario is 4*R*-hydroxyl-L-proline, which is a commonly observed unnatural amino acid in different organisms⁵²⁻⁵⁴. The exact timing and substrate of this plethora of hydroxylation enzymes will be determined in subsequent efforts through a combination of A domain activation assays, genetic knockouts of the candidate oxygenases and *in vitro* biochemical investigation

In addition to L-homotyrosine and L-ornithine, **1** contains the nonproteinogenic amino acid 3*S*-hydroxyl-4*S*-methyl-L-proline, which is presumably derived from 4*S*-methyl-L-proline. Previous studies of **4**,⁴³ nostopeptolide,⁵⁵ and nostocyclopeptide⁵⁶ biosyntheses showed that 4-methyl-L-proline originates from C γ oxidation and subsequent cyclization of L-leucine. Oxidation of L-leucine to 5-hydroxyl-L-leucine was recently identified to be catalyzed by a non-heme iron, α -ketoglutarate dependent oxygenase in *Nostoc punctiforme*.⁵⁷ Thus, it is probable that one of the non-heme, α -ketoglutarate dependent oxygenase such as EcdG, EcdK and HtyE can perform this reaction. However, both the *ecd* and *hty* clusters do not harbor the genes encoding enzymes involved in the reactions downstream to oxidation of L-leucine. A genome-wide search for genes for pyrroline-5-carboxylate (P5C) reductase homolog, proposed to catalyze the final step of 4-methyl-L-proline biosynthesis,⁵⁵ revealed the presence of four candidate genes in *E. rugulosa*. However, an ortholog for each of the four candidate genes are also present in *A. nidulans* A4 (Table S5) so at present it is not yet clear which, if any, is involved in synthesis of the 4*S*-methyl-L-proline for **1**.

In conclusion, we report the discovery of the biosynthetic gene cluster of **1**, the first such cluster for a member of the medically relevant fungal lipopeptide family of compounds. This study has also uncovered the genetic basis for the biosynthesis of the nonproteinogenic L-homotyrosine. The mechanism and timing of the hydroxylation of the residues

Lhomotyrosine, L-proline, 4*S*-methyl-L-proline and L-ornithine, are intriguing features of the biosynthesis of **1** and are currently under investigation in our groups.

MATERIALS AND METHODS

General Methods and Material

E. rugulosa (*A. nidulans* var. *roseus*) strain NRRL 11440 was obtained from Agricultural Research Services Culture Collection (Peoria, IL). Authentic standard for **1** was purchased from Santa Cruz Biotechnology, Inc (Santa Cruz, CA). Primers used in this study were ordered from Integrated DNA Technologies and are listed in Table S7. Sequencing of heterologous expression constructs and knockout cassettes was performed by Laragen, Inc (Culver City, CA). RNA for cDNA amplification was isolated using RiboPure-Yeast Kit from Ambion. First strand cDNA synthesis was performed using SuperScript III- First Strand Synthesis SuperMix (Invitrogen Corp.).

Illumina Hiseq2000 Sequencing and Bioinformatic Analysis

The genomic DNA for sequencing was isolated as described elsewhere from stationary liquid cultures.⁵⁸ Shotgun sequencing was performed at Ambry Genetics (Aliso, Viejo, CA) using Illumina Hiseq 2000 with a read size of 157 bases resulting in a total of ~17 Gbp reads. The Illumina sequencing reads were assembled using a hierarchical assembly method using the assembly programs SOAPdeNOVO⁵⁹ and GeneiousTM and performed by the UCLA Hoffman Cluster. First, the ~17 Gbp total reads were assembled using SOAPdeNOVO using k-mer size of 87 bp. The first-tier contigs were then assembled using Geneious to generate 433 second tier contigs with a N50 of 235,313 and total length of ~32 Mb.

The second-tier contigs were converted to BLAST database format for local BLAST search using stand-alone BLAST software (v. 2.2.18). Gene predictions were performed using the FGENESH program (Softberry) and manually checked by comparing with homologous gene/proteins in the GenBank database. Functional domains in the translated protein sequences were predicted using Conserved Domain Search (NCBI) or InterProScan (EBI). The nucleotide sequences for the *ecd* and *hty* gene clusters are deposited to Genbank database with accession numbers JX421685 and JX421684, respectively.

Fungal Transformation and Gene Disruption

Polyethylene glycol-mediated transformation of *E. rugulosa* NRRL 11440 was performed as done previously³¹ with the following modifications: the spores from two plates were grown in 250 mL GMM with 10 mM ammonium tartrate as sole nitrogen source for 16 hrs at 250 rpm, 28°C and 1 g of the germlings from the culture was used for digestion using 3 g of Vinotaste Pro enzyme mixture (Novozyme). The glufosinate resistance gene *bar* with an upstream *tpc* promoter was amplified from pBARGPE1 plasmid obtained from the Fungal Genetic Stock Center (Kansas City, MO). Glufosinate used for the selection of transformants was prepared by extracting twice with equal volume of 1-butanol from commercial herbicide Finale(Bayer), which contains 11.33% (w/v) glufosinate-ammonium.⁶⁰ Construction of the knockout cassette was performed by fusion PCR as described elsewhere.²⁵ Fungal genomic DNA from the transformants was isolated using ZR-Fungal/Bacterial DNA Miniprep Kit (Zymo). Primers used for PCR screening are listed in Table S7.

Extraction and Characterization of **1**

The echinocandin extraction method is based on US Patent #4,288,549.⁷ Briefly, the strain was grown in Medium 2 [2.5% (w/v) glucose (Sigma), 1% peptone (BD Biosciences), 1% (w/v) starch (Sigma), 1% (w/v) molasses, 0.4% (w/v) N-Z Amine A (Sheffield Biosciences), 0.2% (w/v) calcium carbonate (Sigma)] in 28°C for 7 days in 10 mL cultures for screening of transformants and 2 L for large scale compound extraction. An equal volume of methanol was added to the whole fermentation broth and the mixture was shaken at 16°C for 1 hour. The mixture was then filtered and the pH adjusted to 4.0. The filtrate was extracted twice with equal volumes of chloroform. The concentrated extract was purified using Sephadex LH-20 resin using 1:1 methanol and chloroform solvent system. The fractions containing **1**, determined by LCMS, was further purified using HPLC with C-18 column and a 40–95%, 20 minute water:acetonitrile gradient. Purified **1** was further characterized via Agilent 6520 high-resolution QTOF/LC-MS and its 1D-¹H NMR, 2D-COSY, HSQC and HMBC spectra were recorded using a Varian 600 MHz NMR spectrometer.

Anti-*Candida* Assay

$\Delta ecdA$ and $\Delta htyA$ mutants were grown in 10 mL of liquid Medium 2 at static conditions for 7 days at 28°C. Discs of 10 mm in diameter were cut from the fungal mat and transferred to yeast extract-peptone-dextrose (YPD) agar plates that were previously inoculated with *Candida albicans* ATCC 90234. The co-cultures were grown at 28°C overnight. For chemical complementation of $\Delta htyA$ (Figure S1), L-homotyrosine (0.1 mg/mL) was fed to the static liquid cultures at day-4 before transferring the mycelial discs from individual clones to the YPD plate pre-inoculated with *C. albicans* at day-7.

Cloning of EcdA-M1

The C-terminal boundary of EcdA- T₁ was predicted through alignment of gramicidin synthetase PCP (accession: 1DNY) and fungal NRPSs with EcdA by ClustalW. EcdA-M₁ was amplified from *E.rugulosa* cDNA sample using the primer pair *NdeI*-EcdA-T₀ and *EcoRI*-EcdA-T₁ (See Table S7). The amplicon was gel-purified, digested with *NdeI* and *EcoRI* and ligated into pET28a expression vector to create pET28a-EcdA-M1. QuikChange I Site-Directed Mutagenesis Kit (Agilent Technologies) was used to clone the EcdA-M1 variants using pET28a-EcdA-M1 as template and *ecdA*-S47A-F and *ecdA*-S47A-R as primer pair to create S47A variant and *ecdA*-S1127A-F and *ecdA*-S1127A-R primer pair to create S1127A variant.

Cloning of EcdI

EcdI cDNA was amplified from *E. rugulosa* cDNA sample using primers EcdI-*NdeI*-F and EcdI-*EcoRI*-R. The amplicon was ligated into PCR-blunt vector and was transformed into TOP10 cells. The plasmid was sequenced to confirm correct splicing of the transcript. The plasmid bearing the correct sequence was digested with *NdeI* and *EcoRI* and the insert was cloned into pET28a vector to create pET28a-EcdI.

Heterologous expression of EcdA-M1 and EcdI

pET28a-EcdA-M1 or pET28a-EcdI was transformed into BL21 (DE3) and the cells were grown in 500 mL LB at 37°C and 250 rpm. When the OD₆₀₀ reading reached 0.4, the cultures were cooled to 16°C and protein expression was induced by addition of 60 μM IPTG. After 16 hr of shaking at 16°C, the cells were pelleted and resuspended in Buffer A (50 mM Tris-HCl, pH 7.9, 5 mM NaCl, 1 mM DTT) with 20 mM imidazole. The cells were lysed via sonication and centrifuged at 4°C at 15000 rpm. Nickel-NTA resin was added to the supernatant and was gently stirred at 4°C for 2 hours. The protein/resin mixture was loaded into a gravity flow column and the His-tagged proteins were purified with increasing

concentration of imidazole in Buffer A. Additional anion exchange column purification for EcdI in was performed using a 80 minute gradient of 0–100% Buffer A and Buffer B (50 mM Tris-HCl, 1 M NaCl, 2mM DTT) using a MonoQ 10/100L Anion exchange column (GE Healthcare Life Sciences). The fractions containing the desired protein were concentrated using ultrafiltration column (100 kDa cutoff, for EcdA-M1 and 30 kDa cutoff for EcdI). Protein concentration was determined via by UV absorbance at $\lambda=280$ nm.

ATP-[³²P]PPi Exchange Assays

A typical reaction mixture (500 μ L) contained 1.0 μ M EcdA, 2 mM amino acid substrate (unless specified), 5 mM ATP, 10 mM MgCl₂, 5 mM Na[³²P]-pyrophosphate (PPi) ($\sim 1.8 \times 10^6$ cpm/mL), and 50 mM Tris-HCl (pH 8). Mixtures were incubated at ambient temperature for regular time intervals (e.g., 5 min), and 150 μ L aliquots were removed and quenched with 500 μ L of a charcoal suspension (100 mM NaPPi, 350 mM HClO₄, and 16 g/L charcoal). The mixtures were vortexed and centrifuged at 13000 rpm for 3 min. Pellets were washed twice with 500 μ L of wash solution (100 mM NaPPi and 350 mM HClO₄). Each pellet was resuspended in 500 μ L wash solution and added to 10 mL Ultima Gold scintillation fluid. Charcoal-bound radio-activity was measured using a Beckman LS 6500 scintillation counter.

Loading of [¹⁴C]-substrate onto NRPS

The assay was carried out in two steps. First, a 50 μ L reaction containing 10 μ M EcdA-M1, 20 μ M Sfp, 1mM CoA, 10 mM MgCl₂, 1 mM TCEP, and 50 mM HEPES (pH 7.0) was incubated at ambient temperature for 30 min to convert *apo* EcdA-M1 to its holoform. Afterwards, 8 μ M EcdI, 5 mM ATP, and ~ 40 μ M [¹⁴C]-substrate ($\sim 4.4 \times 10^6$ cpm/mL) were added and incubated for 30 min. The reaction was quenched by 600 μ L acetonitrile for the assays with [¹⁴C]-acyl substrate or 600 μ L 10% trichloroacetic acid for [¹⁴C]-L-ornithine with addition of 100 μ L of 1 mg/mL BSA. The mixture was vortexed and centrifuged at 13,000 rpm for 3 min. The pellet was then washed twice with 600 μ L acetonitrile, dissolved in 250 μ L formic acid, added into 10 mL Ultima Gold scintillation fluid and subjected to a Beckman LS 6500 scintillation counter.

Supplementary Material

Refer to Web version on PubMed Central for supplementary material.

Acknowledgments

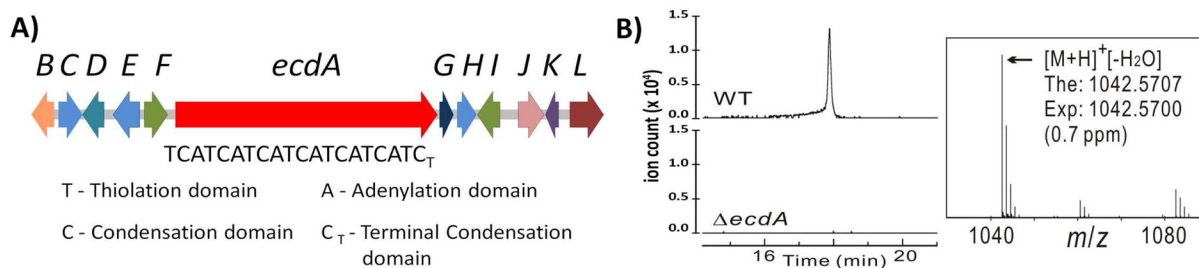
This work is supported by NIH Grants 1R01GM092217 and 1DP1GM106413 to Y. T.; 1R01GM49338 to C.T.W.; and NRSA GM08496 to R.A.C. Genome assembly of *E.rugulosa* NRRL 11440 was performed on the UCLA Academic Technological Services (ATS) Hoffman2 cluster. We would like to thank Qiyang Hu for his assistance in the use of the UCLA Hoffman cluster, Dr. Jaelyn M. Winter for assistance in RNA extraction and Prof. Scott G. Filler from the UCLA Harbor Medical Center for providing the *C. albicans* strain.

References

1. Vincent JL, Rello J, Marshall J, Silva E, Anzueto A, Martin CD, Moreno R, Lipman J, Gomersall C, Sakr Y, Reinhart K. JAMA. 2009; 302:2323. [PubMed: 19952319]
2. Arendrup MC. Curr Opin Crit Care. 2010; 16:445. [PubMed: 20711075]
3. Mayr A, Aigner M, Lass-Flörl C. Mycoses. 2012; 55:27. [PubMed: 21668518]
4. Andes DR, Safdar N, Baddley JW, Playford G, Reboli AC, Rex JH, Sobel JD, Pappas PG, Kullberg BJ. Clin Infect Dis. 2012; 54:1110. [PubMed: 22412055]
5. Kett DH, Shorr AF, Reboli AC, Reisman AL, Biswas P, Schlamm HT. Crit Care. 2011; 15:R253. [PubMed: 22026929]

6. Benz F, Knusel F, Nuesch J, Treichler H, Voser W, Nyfeler R, Keller-Schierlein W. *Helv Chim Acta*. 1974; 57:2459. [PubMed: 4613708]
7. Boeck, L.; Kastner, R. Patent, U S. Eli Lilly and Company; United States: 1981.
8. Schwartz RE, Sesin DF, Joshua H, Wilson KE, Kempf AJ, Goklen KA, Kuehner D, Gailliot P, Gleason C, White R, Inamine E, Bills G, Salmon P, Zitano L. *J Antibiot (Tokyo)*. 1992; 45:1853. [PubMed: 1490876]
9. Mizuno K, Yagi A, Satoi S, Takada M, Hayashi M. *J Antibiot (Tokyo)*. 1977; 30:297. [PubMed: 324959]
10. Strobel GA, Miller RV, Martinez-Miller C, Condrón MM, Teplow DB, Hess WM. *Microbiology*. 1999; 145(Pt 8):1919. [PubMed: 10463158]
11. Roy K, Mukhopadhyay T, Reddy GC, Desikan KR, Ganguli BN. *J Antibiot (Tokyo)*. 1987; 40:275. [PubMed: 3570979]
12. Boeck LD, Fukuda DS, Abbott BJ, Debono M. *J Antibiot (Tokyo)*. 1989; 42:382. [PubMed: 2708131]
13. Debono M, Abbott BJ, Fukuda DS, Barnhart M, Willard KE, Molloy RM, Michel KH, Turner JR, Butler TF, Hunt AH. *J Antibiot (Tokyo)*. 1989; 42:389. [PubMed: 2708132]
14. Debono M, Turner WW, LaGrandeur L, Burkhardt FJ, Nissen JS, Nichols KK, Rodriguez MJ, Zweifel MJ, Zeckner DJ, Gordee RS, Tang J, Parr TR. *J Med Chem*. 1995; 38:3271. [PubMed: 7650681]
15. Bouffard FA, Zambias RA, Dropinski JF, Balkovec JM, Hammond ML, Abruzzo GK, Bartizal KF, Marrinan JA, Kurtz MB, McFadden DC, Nollstadt KH, Powles MA, Schmatz DM. *J Med Chem*. 1994; 37:222. [PubMed: 8295208]
16. Tomishima M, Ohki H, Yamada A, Takasugi H, Maki K, Tawara S, Tanaka H. *J Antibiot (Tokyo)*. 1999; 52:674. [PubMed: 10513849]
17. Joseph JM, Kim R, Reboli AC. *Expert Opin Pharmacother*. 2008; 9:2339. [PubMed: 18710358]
18. Hensens OD, Liesch JM, Zink DL, Smith JL, Wichmann CF, Schwartz RE. *J Antibiot (Tokyo)*. 1992; 45:1875. [PubMed: 1490878]
19. Leonard WR Jr, Belyk KM, Conlon DA, Bender DR, DiMichele LM, Liu J, Hughes DL. *J Org Chem*. 2007; 72:2335. [PubMed: 17343416]
20. Kurokawa N, Ohfuné Y. *J Am Chem Soc*. 1986; 108:6043. [PubMed: 22175373]
21. Evans DA, Weber AE. *J Am Chem Soc*. 1987; 109:7151.
22. Kurokawa N, Ohfuné Y. *Tetrahedron*. 1993; 49:6195.
23. Toth V, Nagy CT, Miskei M, Pócsi I, Emri T. *Folia Microbiol (Praha)*. 2011; 56:381. [PubMed: 21858538]
24. Galagan JE, Calvo SE, Cuomo C, Ma LJ, Wortman JR, Batzoglou S, Lee SI, Basturkmen M, Spevak CC, Clutterbuck J, Kapitonov V, Jurka J, Scaccocchio C, Farman M, Butler J, Purcell S, Harris S, Braus GH, Draht O, Busch S, D'Enfert C, Bouchier C, Goldman GH, Bell-Pedersen D, Griffiths-Jones S, Doonan JH, Yu J, Vienken K, Pain A, Freitag M, Selker EU, Archer DB, Penalva MA, Oakley BR, Momany M, Tanaka T, Kumagai T, Asai K, Machida M, Nierman WC, Denning DW, Caddick M, Hynes M, Paoletti M, Fischer R, Miller B, Dyer P, Sachs MS, Osmani SA, Birren BW. *Nature*. 2005; 438:1105. [PubMed: 16372000]
25. Gao X, Chooi YH, Ames BD, Wang P, Walsh CT, Tang Y. *J Am Chem Soc*. 2011; 133:2729. [PubMed: 21299212]
26. Chiang YM, Szewczyk E, Nayak T, Davidson AD, Sanchez JF, Lo HC, Ho WY, Simityan H, Kuo E, Praseuth A, Watanabe K, Oakley BR, Wang CC. *Chem Biol*. 2008; 15:527. [PubMed: 18559263]
27. Wiest A, Grzegorski D, Xu BW, Goulard C, Rebuffat S, Ebole DJ, Bodo B, Kenerley C. *J Biol Chem*. 2002; 277:20862. [PubMed: 11909873]
28. Marahiel MA, Stachelhaus T, Mootz HD. *Chem Rev*. 1997; 97:2651. [PubMed: 11851476]
29. Rottig M, Medema MH, Blin K, Weber T, Rausch C, Kohlbacher O. *Nucleic Acids Res*. 2011; 39:W362. [PubMed: 21558170]
30. Gao X, Haynes SW, Ames BD, Wang P, Vien L, Walsh CT, Tang Y. *Nat Chem Biol*. 2012; 10:1038. doi:10.1038/nchembio.1047

31. Szewczyk E, Nayak T, Oakley CE, Edgerton H, Xiong Y, Taheri-Talesh N, Osmani SA, Oakley BR. *Nat Protoc.* 2006; 1:3111. [PubMed: 17406574]
32. Nayak T, Szewczyk E, Oakley CE, Osmani A, Ukil L, Murray SL, Hynes MJ, Osmani SA, Oakley BR. *Genetics.* 2006; 172:1557. [PubMed: 16387870]
33. Kraas FI, Helmetag V, Wittmann M, Strieker M, Marahiel MA. *Chem Biol.* 2010; 17:872. [PubMed: 20797616]
34. Chooi YH, Tang Y. *Chem Biol.* 2010; 17:791. [PubMed: 20797606]
35. Hansen DB, Bumpus SB, Aron ZD, Kelleher NL, Walsh CT. *J Am Chem Soc.* 2007; 129:6366. [PubMed: 17472382]
36. Wittmann M, Linne U, Pohlmann V, Marahiel MA. *FEBS J.* 2008; 275:5343. [PubMed: 18959760]
37. Baltz RH, Miao V, Wrigley SK. *Nat Prod Rep.* 2005; 22:717. [PubMed: 16311632]
38. Mootz HD, Finking R, Marahiel MA. *J Biol Chem.* 2001; 276:37289. [PubMed: 11489886]
39. Stachelhaus T, Huser A, Marahiel MA. *Chem Biol.* 1996; 3:913. [PubMed: 8939706]
40. Stachelhaus T, Mootz HD, Bergendahl V, Marahiel MA. *J Biol Chem.* 1998; 273:22773. [PubMed: 9712910]
41. Pfeifer BA, Admiraal SJ, Gramajo H, Cane DE, Khosla C. *Science.* 2001; 291:1790. [PubMed: 11230695]
42. Gadow A, Vater J, Schlumbohm W, Palacz Z, Salnikow J, Kleinkauf H. *Eur J Biochem.* 1983; 132:229. [PubMed: 6188612]
43. Adefarati AA, Giacobbe RA, Hensens OD, Tkacz JS. *J Am Chem Soc.* 1991; 113:3542.
44. Underhill EW. *Can J Biochem.* 1968; 46:401. [PubMed: 5658141]
45. Harimoto Y, Hatta R, Kodama M, Yamamoto M, Otani H, Tsuge T. *Mol Plant Microbe Interact.* 2007; 20:1463. [PubMed: 17990954]
46. Zhang S, Schwelm A, Jin H, Collins LJ, Bradshaw RE. *Fungal Genet Biol.* 2007; 44:1342. [PubMed: 17683963]
47. Scherlach K, Sarkar A, Schroeckh V, Dahse HM, Roth M, Brakhage AA, Horn U, Hertweck C. *ChemBioChem.* 2011; 12:1836. [PubMed: 21698737]
48. Lo HC, Entwistle R, Guo CJ, Ahuja M, Szewczyk E, Hung JH, Chiang YM, Oakley BR, Wang CCC. *J Am Chem Soc.* 2012; 134:4709. [PubMed: 22329759]
49. Xie X, Meehan MJ, Xu W, Dorrestein PC, Tang Y. *J Am Chem Soc.* 2009; 131:8388. [PubMed: 19530726]
50. Ames BD, Nguyen C, Bruegger J, Smith P, Xu W, Ma S, Wong E, Wong S, Xie X, Li JWH, Vederas JC, Tang Y, Tsai SC. *Proc Natl Acad Sci U S A.* 2012; 109:11144. [PubMed: 22733743]
51. Hutton JJ Jr, Kaplan A, Udenfriend S. *Arch Biochem Biophys.* 1967; 121:384. [PubMed: 6057106]
52. Petersen L, Olewinski R, Salmon P, Connors N. *Appl Microbiol Biotechnol.* 2003; 62:263. [PubMed: 12883873]
53. Lawrence CC, Sobey WJ, Field RA, Baldwin JE, Schofield CJ. *Biochem J.* 1996; 313(Pt 1):185. [PubMed: 8546682]
54. Hausinger RP. *Crit Rev Biochem Mol Biol.* 2004; 39:21. [PubMed: 15121720]
55. Luesch H, Hoffmann D, Hevel JM, Becker JE, Golakoti T, Moore RE. *J Org Chem.* 2003; 68:83. [PubMed: 12515465]
56. Becker JE, Moore RE, Moore BS. *Gene.* 2004; 325:35. [PubMed: 14697508]
57. Hibi M, Kawashima T, Sokolov P, Smirnov S, Kodera T, Sugiyama M, Shimizu S, Yokozeki K, Ogawa J. *Appl Microbiol Biotechnol.* 2012 (in press). 10.1007/s00253
58. Carlson JE, Tulsieram LK, Glaubitz JC, Luk VWK, Kauffeldt C, Rutledge R. *Theor Appl Genet.* 1991; 83:194.
59. Li R, Zhu H, Ruan J, Qian W, Fang X, Shi Z, Li Y, Li S, Shan G, Kristiansen K, Yang H, Wang J. *Genome Res.* 2010; 20:265. [PubMed: 20019144]
60. Hays S, Selker E. *Fungal Genet Newl.* 2000; 47:107.

**Figure 1.**

Identification of the *ecd* gene cluster. **A)** Organization of the *ecd* gene cluster. *ecdA* encodes for the six-module nonribosomal peptide synthetase. *ecdI* encodes for the linoleyl-AMP ligase responsible for lipo-initiation of EcdA. Also found in the cluster are *ecdG*, *ecdH*, and *ecdK* encoding for proposed hydroxylases; **B)** Metabolic profile of $\Delta ecdA$ mutant shows the loss of production of **1**.

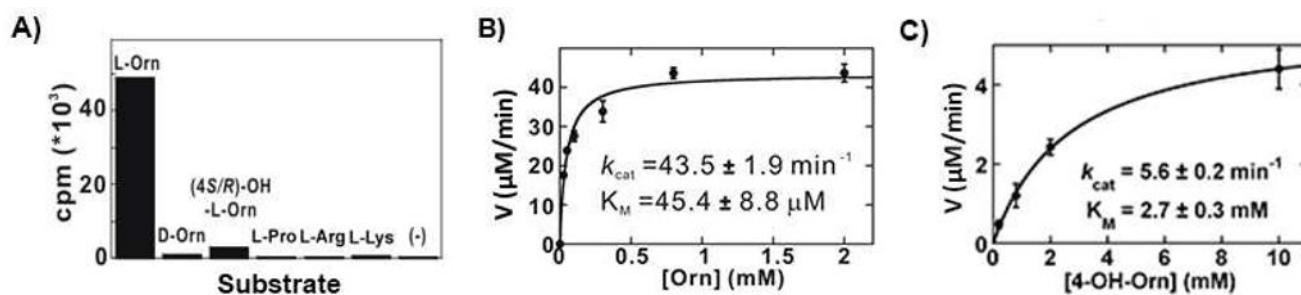


Figure 2. ATP-[³²P]-PPi exchange assay of EcdA-M1 **A)** The adenylation (A) domain of EcdA-M1 shows preference towards L-ornithine **B)** Michaelis-Menten plot for the A domain of EcdA-M1 with L-ornithine as substrate. **C)** Michaelis-Menten plot for the A domain of EcdA-M1 with 4(*R/S*)-OH-L-ornithine as substrate.

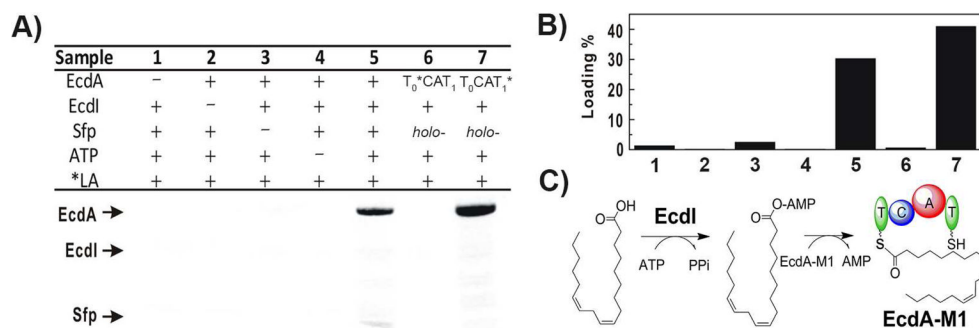


Figure 3. Loading Assay of EcdA-M1. **A)** EcdA-M1, converted to *holo* form *in vitro* by Sfp, is loaded with ¹⁴C-linoleic acid only in the presence of the fatty-acyl-AMP ligase EcdI and ATP as shown in the autoradiogram (lane 5). Loading of EcdA-M1 variants with ¹⁴C-linoleic acid in the same condition as sample 5 **B)** Quantification of percentage of EcdA-M1 loaded with radioactive linoleic acid. Samples 1–7 carried out in identical conditions as in **A**. **C)** Linoleic acid is activated by EcdI to form linoleyl-AMP which is subsequently transferred to EcdA-M1.

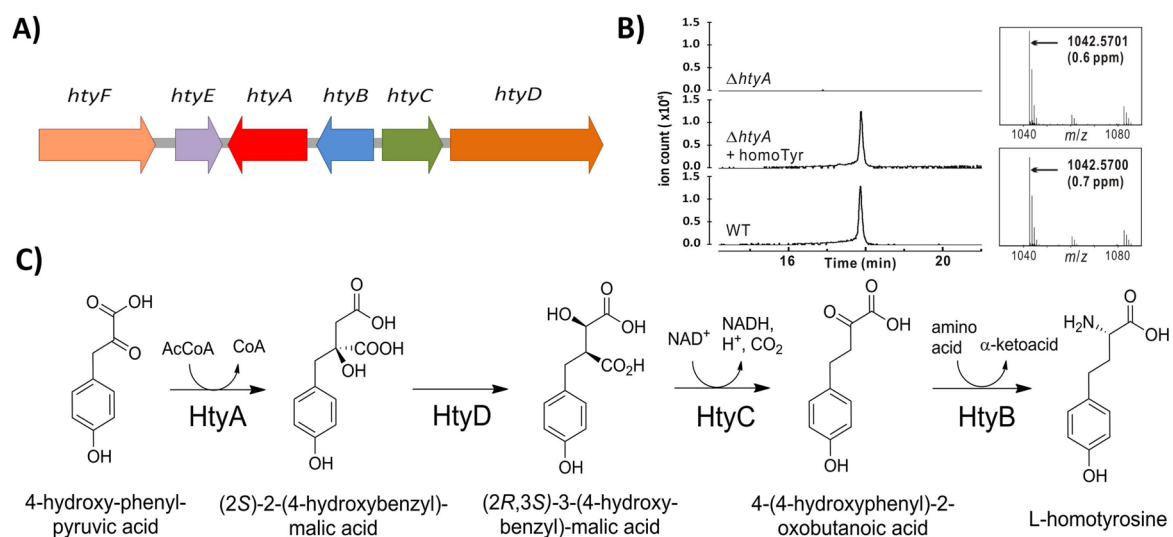
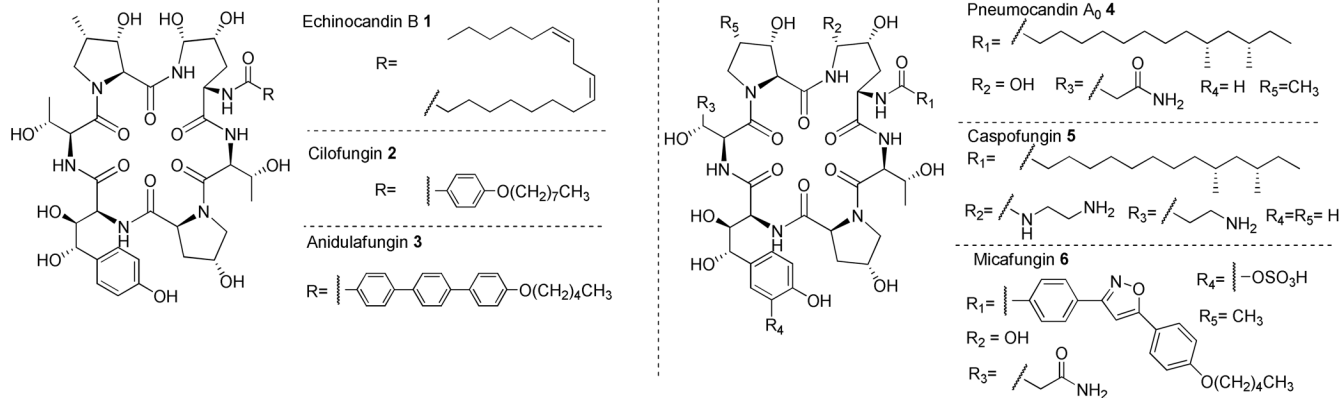
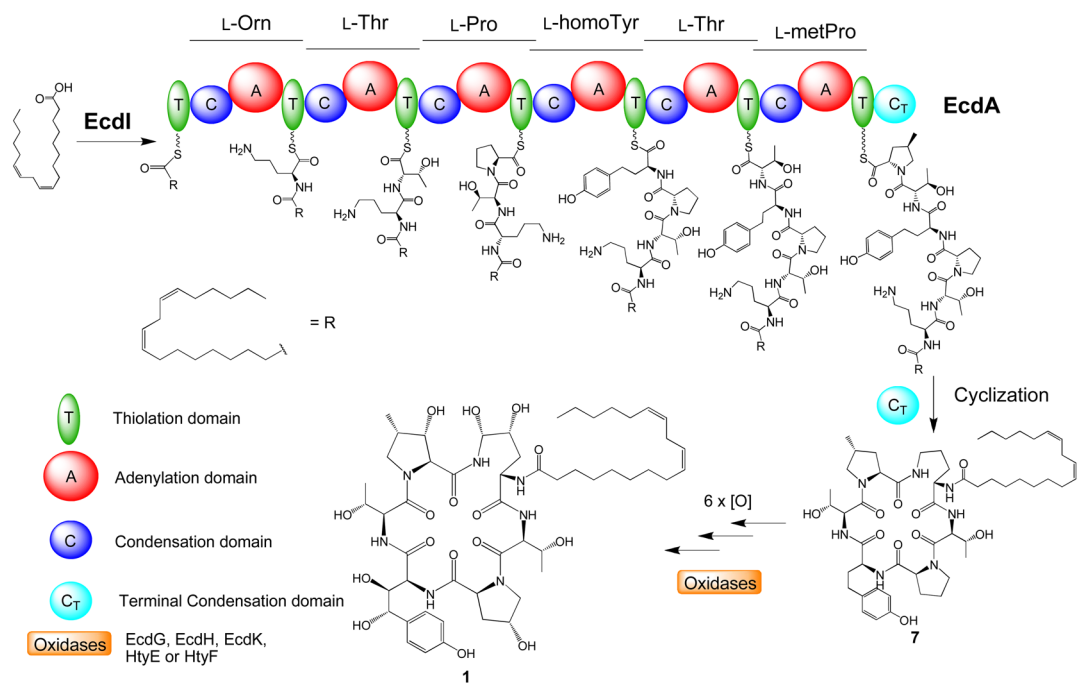


Figure 4. Biosynthesis of L-homotyrosine. **A)** Organization of *hty* gene cluster **B)** Disruption of *htyA* led to the loss of production of **1**, which was restored upon addition of L-homotyrosine to the culture. **C)** Putative biosynthesis of L-homotyrosine.

**Scheme 1.**

Echinocandin B 1 and its semisynthetic derivatives cilofungin 2 and anidulafungin 3. Also shown are the related natural compound Pneumocandin A₀ 4 and its semisynthetic derivatives caspofungin 5 and micafungin 6.



Scheme 2.
Putative biosynthetic pathway of Echinocandin B 1

Table 1

The Echinocandin B Biosynthetic Gene Cluster.

Gene	Length (aa)	Conserved Domain/Function	Nearest BLAST hit (Identity, Similarity)
<i>ecdB</i>	545	fungal transcription factor	<i>A. fumigatus</i> AFUA_048990 (72%, 80%)
<i>ecdC</i>	556	transporter (MFS)	<i>N. fischeri</i> NFIA_042010 (70%, 79%),
<i>ecdD</i>	541	transporter (MFS)	<i>N. fischeri</i> NFIA_042010 (87%, 93%)
<i>ecdE</i>	703	glycosyl hydrolase	<i>N. fischeri</i> NFIA_042050 (78%, 88%)
<i>ecdF</i>	508	glycosidase	<i>P. purpurogenum</i> BAA12320 (71%, 84%)
<i>ecdA</i>	7260	NRPS (T-C-A-T-C-A-T-C-A-T-C-A-T-C-A-T-C-A-T-C)	<i>T. reesei</i> EGR45389(33%, 52%)
<i>ecdG</i>	338	non-heme iron, α -ketoglutarate dependent dioxygenase	<i>C. militaris</i> CCM_03049 (31%, 50%),
<i>ecdH</i>	503	cytochrome P450 heme-iron-dependent oxygenase	<i>N. haematococca</i> 100691 (28%, 48%),
<i>ecdI</i>	559	fatty-acyl- AMP ligase	<i>A. nidulans</i> A4, AN3490 (52%, 67%),
<i>ecdJ</i>	668	hypothetical protein	<i>A. capsulatus</i> 05345 (34%, 47%),
<i>ecdK</i>	332	non-heme iron, α -ketoglutarate dependent dioxygenase	<i>T. reesei</i> TRIREDRAFT_58580 (43%, 63%)
<i>ecdL</i>	1479	multidrug transporter (ABC)	<i>M. anisoplae</i> MAA_01638 (40%, 59%)

Table 2Genes found within the *hty* cluster

Gene	Length (aa)	Conserved Domain/Function	Nearest BLAST hit (Identity, Similarity)
<i>htyF</i>	683	heme-dependent P450 oxygenase	<i>T. stipitatus</i> TSTA_09270 (45%, 64%)
<i>htyE</i>	329	non-heme iron, α -ketoglutarate dependent dioxygenase	<i>A. terreus</i> ATEG09098 (50%, 66%),
<i>htyA</i>	584	isopropyl malate synthase	<i>A. alternata</i> BAI44742 (51%, 68%)
<i>htyB</i>	379	transaminase	<i>A. alternata</i> BAI44740 (55%, 71%),
<i>htyC</i>	366	isopropyl malate dehydrogenase	<i>A. alternata</i> BAI44741 (63%, 73%)
<i>htyD</i>	877	aconitase	<i>A. alternata</i> BAI44743 (57%, 68%),